Energy 207 (2020) 118208

Contents lists available at ScienceDirect

Energy

journal homepage: www.elsevier.com/locate/energy

Production of H_2-rich syngas from excavated landfill waste through steam co-gasification with biochar

Ilman Nuran Zaini [a, *], Yamid Gomez-Rueda [b], Cristina García López [c], Devy Kartika Ratnasari [a], Lieve Helsen [b, d], Thomas Pretz [c], Pär Göran Jönsson [a], Weihong Yang [a]

[a] Department of Materials Science and Engineering, KTH Royal Institute of Technology, Brinellvägen 23, SE-10044, Stockholm, Sweden
[b] Department of Mechanical Engineering, KU Leuven, Celestijnenlaan 300, 3001, Leuven, Belgium
[c] RWTH University Aachen, Department of Processing and Recycling (IAR), 52062, Aachen, Germany
[d] Energyville, Thor Park, Waterschei, Belgium

ARTICLE INFO

Article history:
Received 26 February 2020
Received in revised form
28 May 2020
Accepted 21 June 2020
Available online 30 June 2020

Keywords:
Co-gasification
Landfill waste
Landfill mining
Hydrogen production
Waste to energy
Biomass

ABSTRACT

Gasification of excavated landfill waste is one of the promising options to improve the added-value chain during remediation of problematic old landfill sites. Steam gasification is considered as a favorable route to convert landfill waste into H_2-rich syngas. Co-gasification of such a poor quality landfill waste with biochar or biomass would be beneficial to enhance the H_2 concentration in the syngas, as well as to improve the gasification performance. In this work, steam co-gasification of landfill waste with biochar or biomass was carried out in a lab-scale reactor. The effect of the fuel blending ratio was investigated by varying the auxiliary fuel content in the range of 15–35 wt%. Moreover, co-gasification tests were carried out at temperatures between 800 and 1000 °C. The results indicate that adding either biomass or biochar enhances the H_2 yield, where the latter accounts for the syngas with the highest H_2 concentration. At 800 °C, the addition of 35 wt% biochar can enhance the H_2 concentration from 38 to 54 vol%, and lowering the tar yield from 0.050 to 0.014 g/g-fuel-daf. No apparent synergetic effect was observed in the case of biomass co-gasification, which might cause by the high Si content of landfill waste. In contrast, the H_2 production increases non-linearly with the biochar share in the fuel, which indicates that a significant synergetic effect occurs during co-gasification due to the reforming of tar over biochar. Increasing the temperature of biochar co-gasification from 800 to 1000 °C elevates the H_2 concentration, but decreases the H_2/CO ratio and increases the tar yield. Furthermore, the addition of biochar also enhances the gasification efficiency, as indicated by increased values of the energy yield ratio.

1. Introduction

The Enhanced Landfill Mining (ELFM) concept has been gaining societal interest to replace conventional remediation methods for problematic old landfills. The state-of-the-art of ELFM involves the integration of landfill excavation, advanced materials sorting and processing, and thermal conversion processes for retrieving materials and energy resources back to society [1]. As a result, it may contribute to achieving a closed-loop material cycle, as proposed in the latest circular economy definition [2]. Considering the tremendous number of old landfill sites in EU (at least 500,000 sites [3]), this concept of ELFM has been proposed in various recent EU's policy initiatives. These include European Parliament seminars, briefs, and proposals to the amendment of the Landfill Directive as an alternative strategy to address unwanted implications of landfills while simultaneously reclaiming deposited materials, energy carriers and land resources [4].

Among various thermal conversion methods in the framework of ELFM, high-temperature gasification processes (e.g. slagging gasification) are regarded as viable candidates for combined energy and material valorizations in the form of syngas and vitrified ash residue [5]. Besides, gasification is also favored as it can provide a hydrogen (H_2)-rich syngas when steam is used as the gasifying agent in the process [6]. The use of steam as a gasifying agent also results in products with minimal environmental impacts, such as

* Corresponding author.
E-mail address: zaini@kth.se (I.N. Zaini).

https://doi.org/10.1016/j.energy.2020.118208

Nomenclature and abbreviation

AAEM	alkali and alkaline earth metal
$ash_{815°C}$	the ash content of the initial sample, wt.%
BET	Brunauer-Emmett-Teller
CM	char matrix
daf	dry-ash-free weight basis
ELFM	enhanced landfill mining
EY	energy yield ratio
LHV	lower heating/calorific value
LHV_{fuel}	the calorific value of the fuel/sample, MJ/kg
LHV_{syngas}	the calorific value of the produced syngas, MJ/NM^3
m_i	the initial mass of the sample before gasification, g
m_f	the final mass of the sample after gasification, g
MSW	municipal solid waste
NLDFT	non-local density functional theory
RDF	refuse-derived fuel
SPA	solid-phase adsorption
SPE	solid-phase extraction
V_{syngas}	the total volume of the produced syngas, Nm^3

preventing the formation of NO_x and producing low CO_2 emissions in the gasifier and downstream processes [7–9]. The conversion of landfill waste into H_2 may play a significant role in achieving a circular economy [10].

H_2 has been considered as one of the potential energy carriers of the future [11]. It is gaining a lot of interest due to its flexibility, as it can be used directly as a fuel in fuel cells, internal combustion engines, and gas turbines, or as a medium for chemical energy storage [12,13]. Moreover, H_2 is regarded as the most efficient and environmentally friendly energy carrier due to its high gravimetric energy storage density and ability to produce no harmful emissions during its conversion to electricity [14]. Nowadays, almost 99% of H_2 production still relies on the use of non-renewable sources such as natural gas (76%) and coal (23%) [15]. Hence, new sustainable processes based on renewable sources and waste for H_2 production are highly demanded.

Several studies have demonstrated significant differences between the fuel characteristics of excavated wastes from landfills and fresh Municipal Solid Wastes (MSW) [16,17]. The excavated landfill waste contains typically a high amount of ash, due to the presence of impurities which mainly appear in the form of dirt or soil. It is reported that the excavated waste contains 34–60 wt% of impurities depending on the age of the landfill site and the waste composition [18]. The high amount of impurities, combined with the high volatiles content in the waste, reduces the gasification performance by lowering the thermal output, increasing the ash clinker formation, and producing higher CO_2 emission [19]. It has also been demonstrated that the presence of impurities significantly affects the reactivity of the fuel during steam gasification of landfill waste, where especially a high silica content from the dirt reduces the fuel reactivity [20]. Additionally, the gasification of such waste normally produces a high tar content, which hinders syngas utilization in fuel cells, methanation reactors, and Fischer-Tropsch processes [21]. It also causes blockage of gas downstream, fouling and erosion for equipment [22]. It is known that current routes of tar reduction can be divided by in-situ or ex-situ processes. The in-situ reduction is achieved by adjusting the design and process operation of the gasifiers, as well as by adding additives/catalysts during operation; thus, tar generation inside gasifier is minimized [23]. On the other hand, ex-situ tar reduction does not interfere with the process in the reactor as the tars are removed from the syngas after gasification, through physical processes, chemically treated by thermal and catalytic processes, or partial oxidation [23]. Considering the challenges above, improvements are needed to avoid unwanted problems when landfill waste is used as a gasification feedstock, especially due to the high ash and low carbon contents.

The addition of other fuels has been proposed in several studies to enhance the gasification performance of MSW exhibiting such poor properties. Most of those studies utilized biomass as the auxiliary fuel during the co-gasification of MSW. A study by Pinto et al. [23] concluded that adding biomass is more effective for enhancing the syngas quality from gasification of a low-quality waste fuel (ash > 40 wt%) compared to the addition of natural minerals, as this dilutes the concentration of unwanted components. Moreover, their study observed that additions of biomass during waste gasification in a fluidized bed gasifier enhances the H_2 concentration and lowers the tar yield in the syngas [23]. Cao et al. [24], who investigated the co-gasification of Chinese MSW and pine sawdust at various blending ratios, also found that the H_2 concentration in the syngas increases when adding more sawdust; whereas, the tar yield decreases with the increased amount of sawdust. A similar observation was made in another study in which the addition of wood reduced the tar level during the co-gasification of a mixture of coal, plastic, and wood [25].

In the case of high-temperature MSW gasifications, the slagging gasification technology has been considered as a proven technology for converting ash into slag during gasification of MSW [26]. The state-of-the-art of this technology is similar to that used in blast furnaces in the steel industry, where a high-temperature blast gasifying agent is fed to the bottom part of a shaft furnace. This technology has been implemented widely, especially in Japan and South Korea, where it has been employed and operated continuously at more than 40 commercial plants [27]. Classically, this gasifier relies on the addition of coke as an auxiliary fuel to supply the heat required to maintain the high-temperature gasification and ash melting zones between 1000 and 1800 C [26], as well as maintaining an appropriate gas permeability of the bed. The possibility to replace coke by carbon-neutral resources, such as biochar, as the auxiliary fuel in the gasification process would be intriguing to investigate. Recently, a new 27 million EUR slagging gasification project to treat MSW has been initiated in Singapore where biochar will be used as the auxiliary fuel instead of coke [28]. In this project, a gasification plant with a capacity of 11.5 tons of waste per day has been built based on the aforementioned shaft furnace technology [29]. So far, there is no further information available regarding the related gasification results. Even though the shaft gasifiers above have shown a promising route to convert MSW into syngas and slag, they suffer from the high amount of tar generation. Zhang et al. [30] performed gasification of MSW using a plasma-heated shaft gasifier and found a high amount of tar generation, which is ranged between 20 and 40 wt% of the treated MSW. Therefore, in-situ tar reduction treatments are crucial for these gasifiers.

Biochar is a porous carbon-rich material that can be produced as a byproduct from pyrolysis. It is considered that further utilization of this biochar residue in a gasification process provides a highly beneficial outcome [31]. The steam gasification of biochar has been regarded as a clean way to produce a syngas rich in H_2, which has a higher calorific value [32]. Also, compared to raw biomass, most volatiles has been removed during the transformation to char; thus, the production of problematic tar can be avoided during gasification of biochar [33]. Furthermore, as biochar consists mostly of fixed carbon, its calorific value is significantly higher compared to raw biomass, which may be beneficial to treat high-ash feedstocks. Various aspects of steam gasification of biochar have been reported [33–37]. Zhai et al. [34] investigated the characteristics of rice husk

char gasification with steam. They found that the temperature is the main factor that affects the conversion rate of char, whereas the H_2 content in the syngas is mainly affected by the steam flow rate. In addition, the study could produce a syngas containing nearly 47 vol% of H_2 at 950 C [34]. Steam gasification in a higher temperature range was also conducted by Zhai et al. [35] by using sawdust char. This resulted in an even higher H_2 content of approximately 60 vol% at 1200 C. The utilization of biochar as a secondary fuel for co-gasification has also been proposed, especially in the case of coal gasification [31,38,39]. Yang et al. [38] found that steam co-gasification of blended wheat-straw char and lignite coal produces higher H_2 and CO yields, as well as an increased carbon conversion compared to the gasification of pure coal. The high surface area and high alkali and alkaline earth metal (AAEM) content of the char are the main factors contributing to the positive results [38]. Shen and Murakami [39] added iron-loaded biochar during steam gasification of sub-bituminous coal and found that the H_2 concentration in syngas increases by 20 vol% after the addition of 20 wt% char. Nevertheless, to the best of the authors' knowledge, information regarding the use of biochar in co-gasification of MSW or landfill waste is very limited.

In this study, excavated landfill waste samples were subjected to gasification tests under a steam atmosphere with the main objective to produce a H_2-rich syngas. Biochar was added to enhance the gasification performance, especially in terms of an increased H_2 concentration and a lower tar content in the syngas. Moreover, co-gasification of landfill waste with raw biomass was performed to compare its performance with that of the biochar co-gasification.

2. Materials and methods

2.1. Landfill waste and biomass samples

An excavation project was carried out at the Mont-Saint-Guibert landfill in Belgium, where at least 5.7 million m^3 of waste was deposited between 1958 and 1985. Before the excavation, a geophysical exploration was performed in an area of approximately 2150 m^2. Based on the results of an electrical conductivity analysis, the area was divided into four batches. The material used in this study belongs to the first batch, which represents a total volume of 130 m^3. A two-stage ballistic separation process was then performed by using a commercial scale ballistic separator (STT6000, Stadler Anlagenbau GmbH). The ballistic separator allows the recuperation of fractions that are suitable for the production of refuse-derived fuel (RDF) in addition to other valuable materials, such as inert, glass and metallic materials. The obtained RDF fraction is relatively more homogeneous with a high heating value. Hence, the use of such a machine for the primary sorting process can limit the problems caused by the variability of excavated waste.

As a result of the pretreatment, five fractions were obtained. For the gasification tests in this study, the RDF fraction consisting of the light waste fraction (or commonly also known as a 2D fraction) with a particle size ranging between 90 and 200 mm was chosen as it has the highest calorific value. In dry mass basis, this fraction consists of 1% wood, 4% paper, 8% textile, 43% plastics, 10% other combustible materials, 2% metals, 2% inert materials, and 31% fine particles as was measured by a hand sorting method by García López et al. [40]. Additionally, the particle size of the RDF sample was reduced to a value smaller than 3 mm through a further comminution process. Further details regarding the excavation, sorting, and pre-processing of the landfill waste can be found in a previous study [40]. The samples were then dried in the oven at 105 C for approximately 24 h before the gasification test. This pretreated landfill waste fraction is denoted as "RDF-landfill" throughout the remaining part of this paper.

Lignocellulose sawdust biomass from beech wood was used as the raw biomass sample and the feedstock to produce biochar. This biomass was provided by J. Rettenmaier & Söhne Gmbh, Rosenberg, Germany. A pyrolysis process was carried out to produce biochar by using a vertical lab-scale fixed bed reactor, which consists of a cooling and a heating zone. In the experiment, the biomass was placed inside a metal basket and kept in the cooling zone while the temperature of the heating zone was elevated until 500 C. After it reached this value, the biomass was inserted in the heating zone and this temperature was maintained for 30 min. Thereafter, an evacuation of the basket to the cooling zone took place. The produced biochar was then collected for further gasification tests. The details of the pyrolysis procedure and reactor have been reported by Ratnasari et al. [41].

The fuel compositions of RDF-landfill, biomass, and biochar samples are presented in Table 1. The proximate, ultimate, the calorific value (lower heating value, LHV), and inorganic content measurements were performed by a commercial laboratory (Eurofins Biofuel & Energy Testing Sweden AB, Sweden). The details of the measurement methods can be found in the previous study [20]. The results show that RDF-landfill accounts for a significantly high ash content (46.5 wt%), which is mainly due to the tremendous amount of dirt/soil in the excavated waste sample. In addition, the RDF-landfill sample has a low fixed carbon content (1.8 wt%) due to the high amount of plastics that generally consist of volatile matter instead of fixed carbon. This high amount of plastic also results in a greater calorific value of the RDF-landfill sample (22.9 MJ/kg) compared to the biomass sample (18.3 MJ/kg). On the other hand, the concentration of carbon in biomass was enhanced (from 49.1 to 79.9 wt%) after the pyrolysis process, which results in a 1.8 times higher calorific value of the biochar compared to the original biomass.

Table 1 also shows the composition of the main inorganic contents in the samples. As seen in the table, Si dominates the inorganic contents in the RDF-landfill sample as its amount reaches 16% of the total sample weight. The significant amount of Si mainly comes from the dirt or soil that is attached on the surface of landfill waste materials [20]. Ca accounts for the highest amount among other AAEM species in the RDF-landfill sample, even though its amount is much less significant than Si. In contrast, the inorganic elements in the biomass sample are mainly dominated by Ca, which is followed by K, Mg, Si, Fe, Na, Al. Also, their values are significantly lower than that of RDF-landfill sample. Removing volatile matters of biomass by pyrolysis leads to an increase in the concentration of the inorganic contents in the biochar. As seen in the table, the amount of inorganic contents increase in the case of biochar, and their amounts follow the same order to that of the biomass sample.

2.2. Steam gasification experiments

The steam gasification tests were performed by using a lab-scale horizontal tube reactor, as schematically shown in Fig. 1. The reactor has a total length of 1000 mm and an inner diameter of 25 mm. Blended mixtures of RDF-landfill waste with biomass or biochar, having different mass ratios (85:15, 75:25, and 65:35), were subjected to the gasification tests to investigate the synergistic effect of the fuels. The low biomass/biochar blending ratios (<40 wt%) were chosen as this study focuses on the utilization of those materials as auxiliary fuels; hence, their proportion should not exceed that of the main fuel (RDF-landfill). For each experiment, approximately 4 g of sample was contained in an alumina sample boat which was kept in the cooling zone prior to the gasification reaction. The furnace was heated up until the target temperature (800, 900, or 1000 C) at a constant nitrogen flow of

Table 1
Composition of the RDF-landfill waste, biomass, and biochar used for the steam gasification tests.

Compositions	RDF-Landfill waste	Biomass (beech wood)	Biochar (beech wood char)
Proximate (wt.%, db)			
Volatile matter	55.3	84.2	26.9
Fixed carbon	1.8	15.0	67.3
Ash	46.5	0.8	5.8
Ultimate (wt.%, db)			
C	40.5	49.1	79.9
H	6.1	6.1	2.6
N	1.10	0.12	0.29
O	4.3	43.8	11.4
S	0.234	0.026	0.051
Cl	1.203	<0.01	0.014
LHV (MJ/kg, db)	22.9	18.3	29.6
Inorganic (mg/kg, db)			
Al	17,700	31	172
Ca	29,800	1880	8480
Fe	21,600	93	405
K	4950	1010	4510
Mg	2470	401	1710
Na	2910	63	543
Si	160,000	140	802

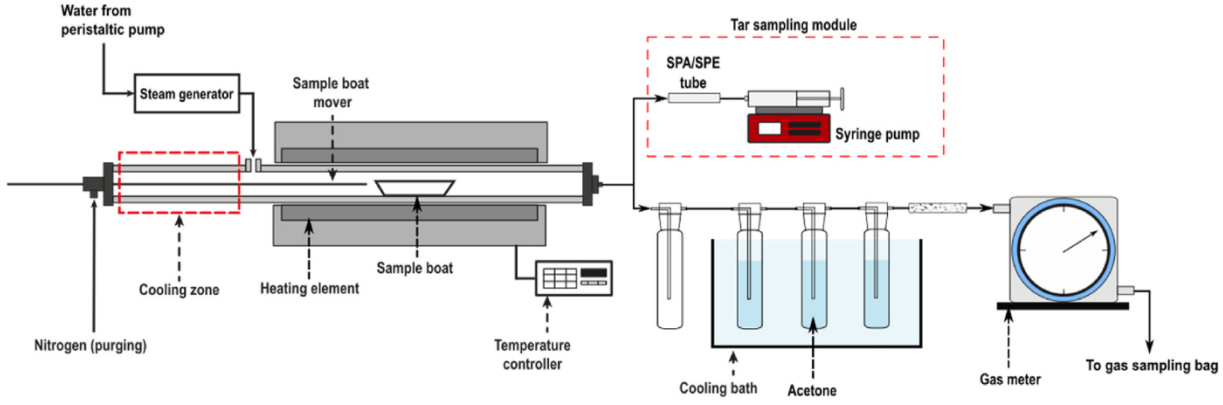

Fig. 1. Schematic diagram of the lab-scale furnace used for gasification tests.

160 ml/min. When the furnace had reached the target temperature, pre-heated steam with a flow rate of approximately 0.5 g/min was introduced to the tube reactor. Thereafter, the sample boat was inserted into the heating zone and the gasification test was maintained at this condition for 30 min. During the reaction, the raw syngas was cooled down to trap the tar content by using a series of impingers filled with acetone and cooled at −15 C. The volume of cleaned syngas was measured by a drum-type gas meter (TG1 type, Ritter, Germany), prior to the gas collection in a 25 L gas sampling bag. After the gasification was completed, the sample boat was withdrawn back to the cooling zone. At the same time the steam flow was shut off, and the nitrogen flow was raised to 320 ml/min for another 30 min to make sure that all syngas was collected. The collected syngas was then analyzed by using a micro-gas-chromatography analyzer (490 Micro GC System QUAD, Agilent) to measure the concentration of H_2, CO, CO_2 and C_xH_y gases (CH_4, C_2H_2, C_2H_4, C_2H_6, C_3H_6, and C_3H_8). Further details of the setup are reported by Sophonrat et al. [42]. Furthermore, the liquid solution which consisted of tar, water, and acetone (contained in the impingers) was collected and filtered through a filter paper (8–10 μm retention size). Subsequently, the filtered liquid solution was heated up for 12 h at 40 C and the tar yield of the gasification was defined as the weight of the remaining dried tar after the evaporation process. For some co-gasification cases, a tar sample was collected during the first 5 min of the reaction, and subsequently analyzed by using the Solid-phase Adsorption - Solid-phase Extraction (SPA/SPE) method developed by KTH [43] to investigate its composition.

2.3. BET analysis of biochar

Brunauer-Emmett-Teller (BET) gas sorptometry measurements were performed by using a Micromeritics model ASAP 2000 instrument to characterize the BET surface area of the raw and gasified biochar samples. The sample was subjected to a degassing process conducted at 250 °C for 12 h before the BET analysis. The test was then performed by using the N_2 isotherm adsorption method on the degassed particles at −196 °C. The pore size distributions of the biochar samples were analyzed by using the non-local density functional theory (NLDFT) method.

2.4. Evaluation of gasification performance

The conversion rate of the feedstock sample was determined after each gasification test by using the following calculation,

$$Conversion\ rate = \frac{m_f - (m_i \cdot ash_{815\ ^\circ C})}{m_i \cdot (1 - ash_{815\ ^\circ C})} \quad (1)$$

where m_i is the initial mass of the sample before the gasification test and m_f is the final mass of the solid residue after the gasification test. Furthermore, $ash_{815\ ^\circ C}$ is the ash content (in wt.%) of the initial sample, which was measured by combustion at 815 C as was also mentioned in Table 1.

In addition, the performance of the gasification tests was assessed by using the energy yield ratio (*EY*), which can be expressed as follows:

$$Energy\ yield\ ratio(EY) = \frac{LHV_{syngas} x V_{syngas}}{LHV_{fuel} x m_i} \quad (2)$$

where, LHV_{syngas} represents the calorific value of the produced syngas (MJ/Nm^3), V_{syngas} is the total volume of produced syngas (Nm^3), and LHV_{fuel} is the calorific value of the fuel (MJ/kg).

3. Results

3.1. Effect of fuel blending on the conversion rate, syngas yield, and tar yield

Fig. 2 presents the conversion rate, syngas yield, and tar yield of steam gasification of RDF-landfill samples with different amounts of biomass or biochar added at a gasification temperature of 800 C. In Fig. 2, the yield values are presented based on the dry ash free weight of the corresponding fuel (g/g-fuel-daf). Moreover, curves that represent the predicted values of product yield were added to evaluate the synergetic behavior in the co-gasification system. Those values were determined based on the weighted average values from separate gasifications of RDF-landfill, biomass, and biochar. Steam gasification of the RDF-landfill sample results in syngas and tar yields of 0.73 and 0.051 g/g-fuel daf, respectively. As can be seen in Fig. 2(a), adding more biomass during steam gasification of RDF-landfill increases the syngas yield, which is caused by the higher volatile and fixed carbon contents of the biomass. In detail, adding biomass elevates the syngas yield up to 0.83 g/g-fuel daf at biomass content of 35 wt%. Moreover, the measured values of the syngas yield are approximately similar to the predicted values at different biomass contents. This indicates an insignificant interaction between landfill waste and biomass during gasification. Furthermore, no significant differences are found on the values of tar yield at low biomass proportions. A notable difference is observed at a biomass share of 35 wt% as the tar yield value is 45% higher than the predicted value. Finally, there are no significant changes in terms of the conversion rate as all values are nearly equal to 1.0 for all cases. This indicates that all samples have been fully converted into syngas and tar within the investigated retention time.

In contrast, steam co-gasification of RDF-landfill with biochar results in different trends with respect to the product yield distribution. Fig. 2(b) shows the yield distribution and fuel conversion rate for different amounts of biochar. As illustrated in Fig. 2(b), tar production in RDF-landfill gasification decreases as biochar is added to the fuel mixture, especially at biochar shares above 25 wt %. In particular, the tar yield decreases by 63 and 72% in the case of biochar shares of 25 and 35 wt%, respectively. These numbers are at least 52% lower than the predicted tar yield for the corresponding biochar contents. This trend indicates that a significant synergetic effect occurs on the tar generation during the co-gasification process. The production of syngas increases following the tar reduction due to the presence of biochar. As can be seen in Fig. 2(b), the total

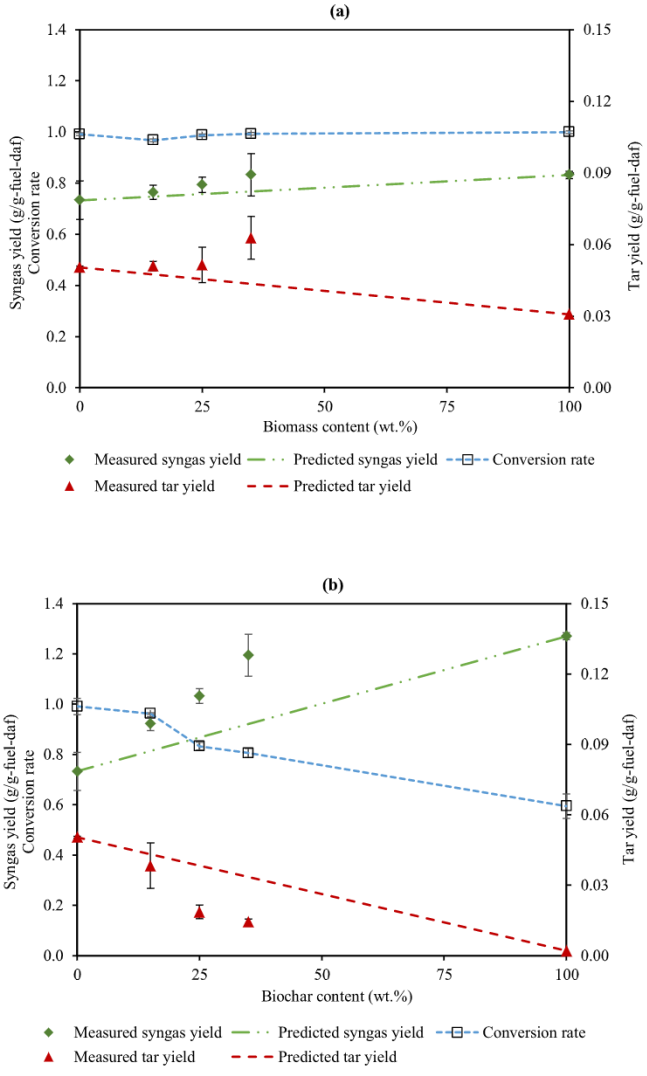

Fig. 2. Product yield distribution and conversion rate of steam gasification of RDF-landfill with different feedstock shares of (a) biomass and (b) biochar at a gasification temperature of 800 C.

mass of syngas raises up to 1.2 g/g-fuel-daf when 35 wt% of biochar is added. Nevertheless, co-gasification of RDF-landfill with biochar suffers a low conversion rate which inversely correlates to the biochar share in the feedstock. Co-gasification with a biochar share of 35 wt% results in the lowest conversion rate (0.81). This is due to the low reactivity of heterogeneous reactions, which occur between char and gasifying agents.

3.2. Effect of fuel blending on the gas yield and concentration

Fig. 3(a–d) illustrate the yield of syngas components resulting from co-gasification of RDF-landfill with biomass. As can be seen in Fig. 3, increasing the biomass share in the fuel mixture results in a higher H_2, CO, and CO_2 yields. Only C_xH_y-gases have lower yields at higher biomass proportions. The measured yield values of those gases are similar to the predicted values which indicates that there are no clear synergetic effects. The increase of the CO and CO_2 yields can mainly be attributed to the fact that biomass fuel contains significantly more oxygen than landfill waste (ten times higher). Meanwhile the lower yield of C_xH_y-gases is caused by the lower

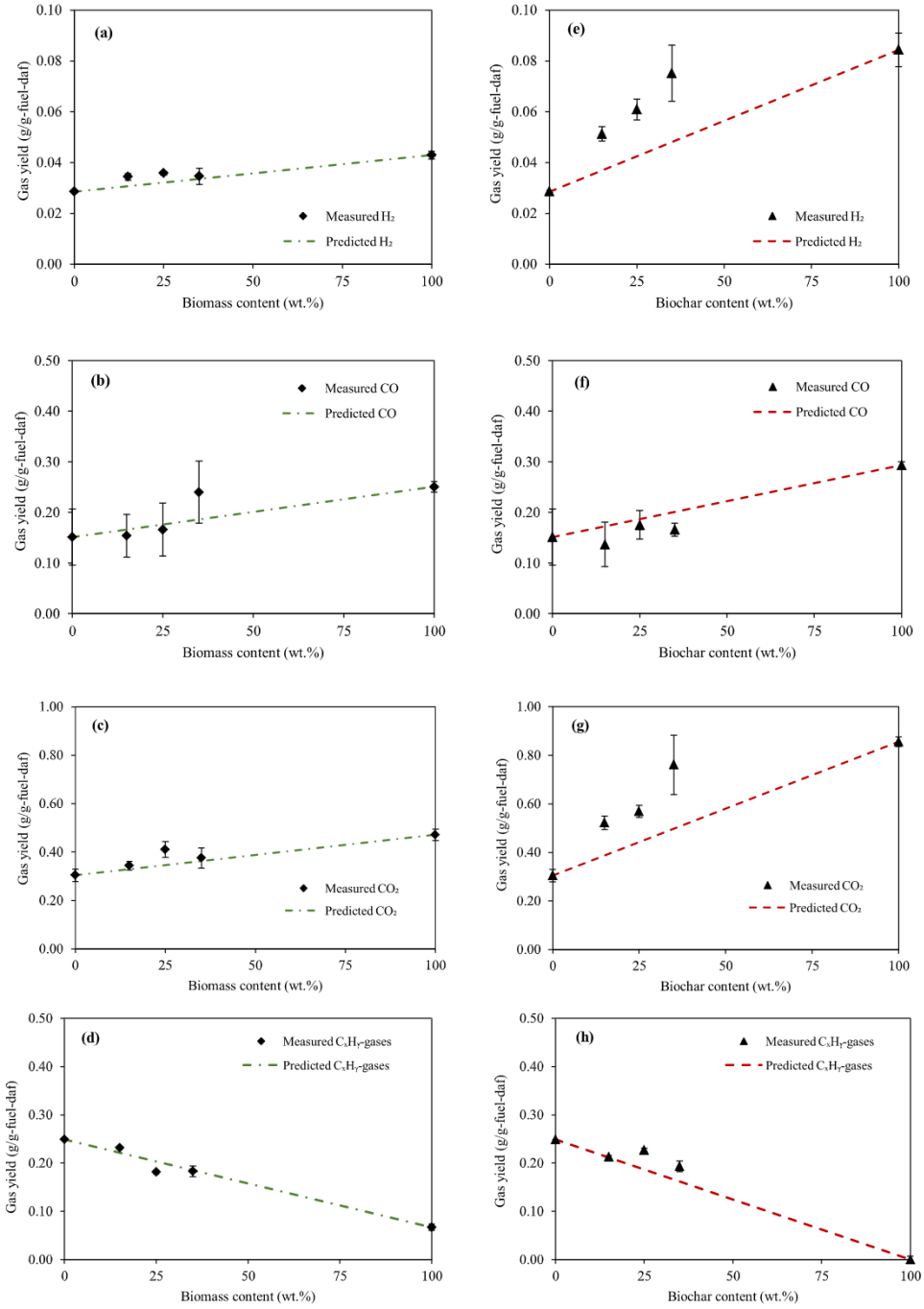

Fig. 3. Gas yield (in g/g-fuel daf) during steam co-gasification of RDF-landfill with biomass (a–d) or biochar (e–f) for different blending proportions at a gasification temperature of 800 C.

concentration of plastic in the waste-biomass mixture. It is known that the presence of plastic polymers accounts for generation of hydrocarbon gases in the syngas. For example, the presence of PE, such as HDPE and LDPE, leads to the production of more ethane, ethene, and n-butane [20].

The composition of syngas (in vol%) produced from co-gasification of RDF-landfill at 800 C with different fuels blending proportions is shown in Table 2. As seen in the table, the concentrations of H_2 and CO_2 increase with increasing biomass proportions. The highest H_2 and CO_2 concentrations are achieved at a biomass content of 25 wt% for which their values are approximately 45 and 23 vol%, respectively. Meanwhile, steam co-gasification with biomass contents of 15 and 25 wt% resulted in lower CO concentrations than gasification of only RDF-landfill; even though the concentration increases at a biomass content of 35 wt%. The concentration of C_xH_y-gases is inversely correlated with the increase of biomass content as its value decreases from 25.6 to 15.9 vol% when the biomass is added at 35 wt%.

The syngas components yield from the co-gasification of RDF-landfill with biochar is presented in Fig. 3(e and f). Fig. 3 demonstrates that there are significant improvements in the H_2 generation when biochar is added to the gasification process. Specifically,

Table 2
Steam gasification results of different fuel mixtures at different gasification temperatures.

Sample no.	Fuel composition (wt.%)			Gasification temp. (C)	Gas concentration (vol%)				H_2/CO	LHV syngas (MJ/Nm^3)	EY ratio
	RDF-landfill	Biomass	Biochar		H_2	CO	CO_2	C_xH_y			
1	100	–	–	800	38.0	17.9	20.1	25.6	2.50	24.0	0.44
2	–	100	–	800	48.2	21.6	22.5	7.7	2.40	16.0	1.03
3	–	–	100	800	56.6	14.1	26.2	3.1	4.04	12.6	0.73
4	85	15	–	800	44.1	14.0	20.1	21.8	3.70	20.7	0.53
5	75	25	–	800	45.2	14.6	23.4	16.8	3.34	18.9	0.55
6	65	35	–	800	42.6	20.6	20.7	15.9	2.11	21.0	0.69
7	85	–	15	800	51.2	9.9	23.7	15.2	5.96	17.1	0.50
8	75	–	25	800	52.6	10.7	22.0	15.6	5.05	16.2	0.59
9	65	–	35	800	53.5	10.4	25.0	11.1	5.36	15.0	0.56
10	100	–	–	900	41.1	11.2	15.5	32.2	4.12	21.6	0.51
11	100	–	–	1000	47.5	10.3	11.7	30.5	4.74	20.5	0.54
12	65	35	–	900	45.5	18.0	18.7	17.8	2.56	19.7	0.80
13	65	35	–	1000	47.9	20.0	15.8	16.3	2.39	18.7	0.84
14	65	–	35	900	54.8	13.8	20.6	10.9	3.98	15.6	0.88
15	65	–	35	1000	55.8	20.1	15.1	9.1	2.78	17.4	1.11

the yield of H_2 is nearly doubled (from 0.029 to 0.051 g/g-fuel-daf) when 15 wt% of biochar is added during co-gasification. Further enhancements are achieved at higher biochar proportions as the production yield increases almost three times (to 0.075 g/g-fuel-daf) for 35 wt% biochar addition. This value is approximately 2.2 times higher than that of co-gasification with 35 wt% of biomass fuel. Furthermore, the value is also 56% higher than the predicted value which indicates a significant synergistic effect on the H_2 production. A similar trend is also observed for CO_2 production as the yield values elevate more than the predicted values and increase at higher biochar contents. For instance, for a biochar content of 35 wt%, the measured CO_2 yield is 53% higher than the predicted yield. In contrast, the production of CO shows a different tendency as the measured yields are not significantly different with that of mono gasification and their values are 6–21% lower than the predicted yields. Furthermore, the C_xH_y gases' yield decreases with the increase of biochar content. At biochar shares of 25 and 35 wt%, the yield values can be seen shift to at least 20% higher than the predicted values.

Overall, the addition of biochar during steam gasification of RDF-landfill produces a syngas with a higher concentration of H_2 compared to biomass co-gasification. At the lowest biochar content of 15 wt%, the syngas contains 51 vol% of H_2. This is nearly 34 and 16% higher than the value from gasification of RDF-landfill only and biomass added at 15 wt%, respectively. The H_2 concentration then gradually increases and reaches a value of 54% for a biochar content of 35 wt%. Similarly, the concentration of CO_2 is also known to increase with an increasing biochar content. In contrast, a significant reduction is found for the CO concentration, which is almost 10 vol % for 15 wt% of biochar in the feedstock, or 45% lower than that of pure RDF-landfill gasification. However, the concentration increases slightly (by less than 1 vol%) for biochar contents of 25 and 35 wt%. Finally, the concentration of C_xH_y-gases behaves in the same way as for a biomass co-gasification. Thus, its value decreases proportionally with an increased in biochar content.

3.3. *Effect of temperature on gasification products*

Fig. 4(a) presents the product characteristics from steam gasification of RDF-landfill without any fuel additions at different temperatures. As can be seen in Fig. 4, raising the gasification temperature from 800 to 1000 C slightly increases the syngas yield from 0.73 to 0.78 g/g-fuel-daf. Furthermore, the H_2 yield is linearly correlated to the gasification temperature, increasing from 0.029 g/g-fuel-daf at a gasification temperature of 800 C to 0.046 g/g-fuel-daf at 1000 C. On the contrary, the CO and CO_2 yield decrease as the gasification temperature increases. Meanwhile, the yield of C_xH_y-gases raises with the increase of gasification temperature. Overall, at 1000 °C, the syngas consists of 47.5 vol% H_2, 10.3 vol% CO, 11.7 vol% CO_2, and 30.5 vol% C_xH_y-gases as can be seen in Table 2.

Steam co-gasification of RDF-landfill containing 35 wt% biomass or biochar were also performed at different temperatures, and the results are presented in Fig. 4(b and c). As can be seen in Fig. 4(b), co-gasification of the landfill waste with biomass exhibits significant reductions in tar yields at higher gasification temperatures. Specifically, there is at least a 45% tar yield reduction when the temperature increases from 800 to 900 C, which is followed by a further reduction of 42% at 1000 C. At these higher temperatures, the tar compounds are cracked into smaller hydrocarbon molecules or non-condensable gases. This contributes to the higher syngas production at higher gasification temperatures, as also can be seen in Fig. 4(b). Correspondingly, the H_2 yield also rises and the highest value of 0.054 g/g-fuel-daf is obtained at 1000 C. This result leads to the H_2 concentration of 47.9 vol% in the syngas. In contrast, gasification at higher temperatures produces lower levels of CO_2 concentrations, decreasing from 21.0 to 15.8 vol% with an increasing temperature from 800 to 1000 C. No clear trend is observed with respect to the concentration of CO and C_xH_y-gases and their relations to the gasification temperatures, as the lowest CO and the highest C_xH_y-gases concentrations are recorded at 900 C.

On the other hand, the co-gasification of the RDF-landfill and biochar at higher temperatures also produce higher H_2 yield values than that of other fuels. Specifically, the H_2 yield increases from 0.075 to 0.111 g/g-fuel-daf, when the temperature is raised from 800 to 1000 C. This result responsible for a H_2 enrichment in the syngas as its concentration elevates from 53.5 to 55.8 vol%. At the same time, the CO yield also increases with the rise of the gasification temperature as its value is 3.4-fold at the same temperature increment. However, a different trend is observed in the case of CO_2 as its yield decreases from 0.761 to 0.662 g/g-fuel-daf with an increasing temperature from 800 to 1000 C. No notable differences were observed in the case of C_xH_y-gases' yield at higher temperatures. Lastly, in contrast to the other fuel mixtures, the production of tar during steam co-gasification of RDF-landfill with biochar exhibits higher yield values at higher gasification temperatures. As can be seen in Fig. 4(c), the tar yield rises to 0.020 and 0.023 g/g-fuel-daf at 900 and 1000 C, respectively, from its initial value of 0.014 g/g-fuel-daf at a temperature of 800 C.

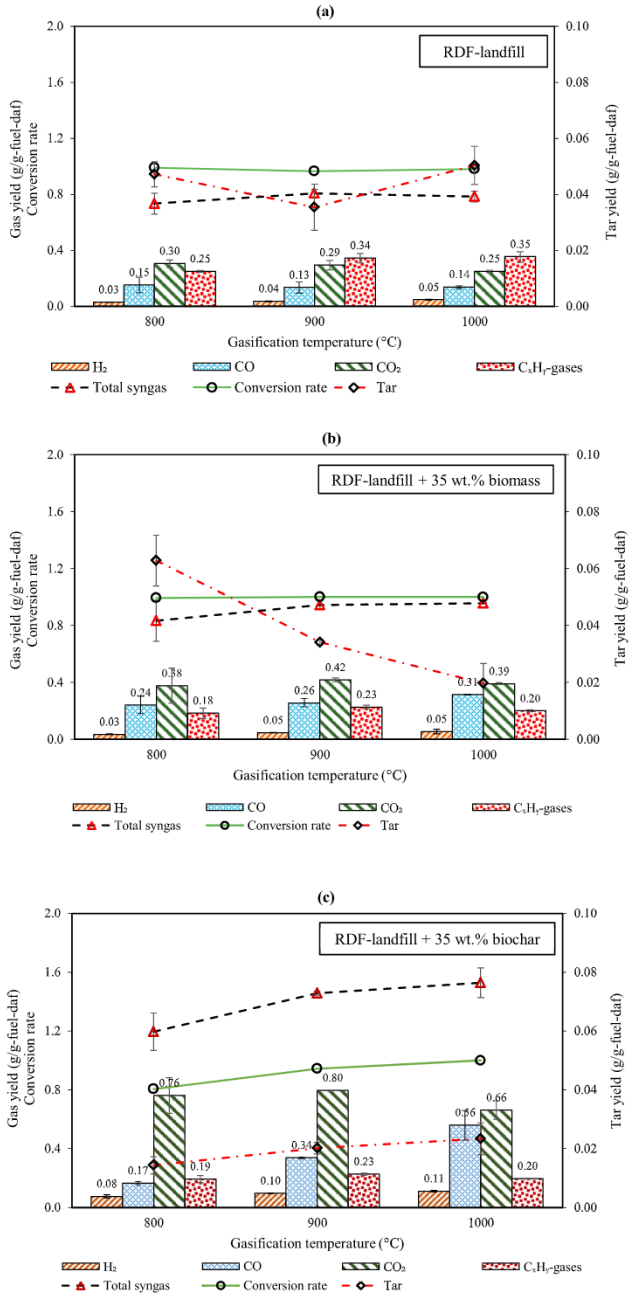

Fig. 4. Products from steam co-gasification of RDF-landfill with (a) no fuel additions, (b) 35 wt% biomass, and (c) 35 wt% biochar at different temperatures.

3.4. H_2/CO ratio

The molar ratio of H_2/CO is a critical parameter to match with the end-use product processing requirements of syngas, such as for methanol, ammonia, and synthetic fuels through Fischer-Tropsch synthesis [44].Table 2 lists the values of these ratios for steam gasification of different fuel mixtures at different gasification temperatures. As can be seen in Table 2, the values of the ratios H_2/CO of the syngas produced from steam gasification of the RDF-landfill in the temperature window 800–1000 C varies between 2.5 and 4.74. A higher gasification temperature favors a higher H_2/CO value.

At 800 C, steam co-gasification of RDF-landfill with biomass at lower blending ratios (<35 wt%) results in higher H_2/CO values compared to that of pure RDF-landfill. However, at a biomass proportion of 35 wt%, the value is found to be lower due to the high CO production originating from the biomass. A significantly higher H_2/CO value (2.4 times higher than in the case without biochar) is observed in the case of co-gasification of RDF-landfill with biochar. Specifically, the H_2/CO ratio ranges between 5.05 and 5.96, where the biochar content of 15 wt% accounts for the highest value.

In contrast to gasification at 800 C, syngas produced during gasification of the RDF-landfill sample only exhibits higher H_2/CO values than that of samples with biomass or biochar addition at higher gasification temperatures. Specifically, the H_2/CO ratio values of the syngas are 4.12 and 4.74 when gasification occurs at 900 and 1000 C, respectively. This is mainly caused by the tendency of lower CO concentration at higher gasification temperatures. Meanwhile, at higher temperatures, gasification of the RDF-landfill with a biochar content of 35 wt% tends to produce a syngas with lower H_2/CO ratio values as the values are 3.98 and 2.78 at 900 and 1000 C, respectively. However, these values are still higher than those of biomass co-gasification at the same temperatures.

3.5. Syngas calorific value and EY ratio

Table 2 also presents the syngas calorific value (LHV) as well as the Energy Yield (EY) ratio achieved through gasification of the different fuel mixtures at different gasification temperatures. As can be seen in Table 2, gasification of the RDF-landfill sample produces a syngas with higher LHV than all co-gasification cases regardless of the gasification temperature. The values varies between 20.5 and 24.0 MJ/Nm^3. This is mainly due to the high concentration of heavy hydrocarbon gases (C_xH_y-gases) present in the syngas produced from landfill waste. For similar reasons, gasification tends to generate a syngas with higher LHV values when biomass is added as the auxiliary fuel compared to biochar regardless the blending ratio and the gasification temperature.

Even though their syngas has a relatively high calorific value, the gasification of RDF-landfill samples suffers from low EY values as a result of a low syngas yield and eminent chemical energy losses in the form of tar. The EY value is 0.44 at a gasification temperature of 800 C, which rises to 0.54 at 1000 C. The use of biomass or biochar as an auxiliary fuel could enhance the gasification performance as indicated by higher EY values. Specifically, at 800 C, one can see that the value of the EY ratio increases proportionally with the amount of biomass content in the fuel, as its maximum value (0.69) is obtained at a biomass content of 35 wt%. In contrast, the optimum EY value in the case of biochar co-gasification is obtained at a 25 wt% biochar content. Greater amounts of biochar reduce the EY value, due to the low conversion rate of biochar at a low gasification temperatures. Nevertheless, co-gasification of 35 wt% biochar exhibits better gasification performance at higher temperatures than that of other fuel mixtures. At 1000 C, this gasification has an EY value of 1.11, whereas gasification of RDF-landfill without any fuel addition and with 35 wt% biomass addition only show EY values of 0.54 and 0.84, respectively.

4. Discussion

The results in Figs. 2–3 demonstrate that no apparent synergetic effects are observed during the co-gasification of RDF-landfill with biomass concerning the H_2 yield. This finding is in contradiction with other studies related to the gasification of such feedstock mixtures. For example, previous studies that investigated the co-gasification of pure plastics and biomass often observed a synergistic effect between them [45–47]. Those studies claimed that

radicals released by one component enhancing decomposition of the other component in the feedstock. Specifically, it begins with the release of volatiles from biomass, which starts before radical formation in plastics [46]. After that, the release of more H and OH radicals from plastics act as hydrogen donor species, promoting the cracking of the aromatic compounds in the biomass [46]. This then typically leads to a higher syngas yield than the predicted value.

The absence of the synergetic effects in this study might be explained by several reasons. The high amount of inorganic materials in the RDF-landfill, especially Si, could be one of the reasons. As mentioned previously, the synergistic effect between plastic and biomass occurs as the biomass typically releases volatiles earlier than that of plastics. At the same time, the release of volatiles from biomass can be affected by the presence of inorganic elements. According to previous studies, the presence of inorganic elements such as Si, could inhibit the devolatilization rate of biomass and cause the degradation of biomass to start at a higher temperature [48,49]. Correspondingly, the release of volatiles from biomass might be delayed due to the addition of high inorganic materials from RDF-landfill. This event then probably causes the disappearance of synergetic effects between plastics and biomass. Furthermore, Si has been known as an inhibitor during steam gasification itself. Rizkiana et al. [50] investigated the effect of adding biomass ash during the steam gasification of a low-rank coal. They found that the presence of Si in the ash could inhibit the reactivity of the sample so that the gasification rate is decreased. This inhibition would eventually lead to the reduction of gas yield, especially H_2 [50]. Therefore, the results of this study suggest that the synergetic effect due to plastic-biomass interaction during co-gasification might be cancelled by the greater effect of inhibition by Si.

Apart from the explanation above, it should be considered that this study only focused on the co-gasification at low biomass proportions ($\leq$35 wt%). There is a possibility that the synergistic effects can only be observed at a high range of biomass proportions. Nevertheless, more investigations should be done to verify the phenomenon mentioned above.

On the other hand, the synergetic effects observed in the case of biochar co-gasification can be explained by the heterogeneous reactions during the tar reforming process over biochar particles. It is known that the rate of heterogeneous tar conversion on the char surface is higher than the homogeneous tar reforming (R4 – R6), especially at temperatures lower than 1000 °C [51]. The main mechanisms of tar reforming over biochar consist of tar adsorption, dehydrogenation to form soot on the char surface, and soot gasification [52]. The performance of these mechanisms is significantly affected by the porosity of biochar. In Fig. 6, it can be noticed that the raw biochar has a relatively low porosity as indicated by the low BET surface area of 10.1 m^2/g. This value is comparable with the BET surface area values for different biochar samples generated from pyrolysis at ±500 °C by previous studies, which include biochar samples made from hornbeam sawdust (32 m^2/g) [53], lignin (9.8 m^2/g) [54], corn straw (9.95 m^2/g) [55], and cotton stalk (11.63 m^2/g) [56].

As illustrated in Fig. 5, the initial process begins when the tar released from the waste particles come into contact with the active sites on the biochar surface. The tar is then adsorbed into the biochar matrix, in which the H_2 is released through polymerization reactions and leaving soot on the char surface (R7) [52]. After that, the soot is consumed by H_2O or CO_2 and transformed into additional gases. This mechanism explains the synergetic effects that occur on the H_2 and total syngas yields during the RDF-biochar co-gasification test, as their measured values are higher than the predicted values and non-linearly increase with the biochar proportion.

Water gas:

$$C + H_2O \rightarrow CO + H_2 \quad (R1)$$

Water gas shift:

$$CO + H_2O \rightarrow CO_2 + H_2 \quad (R2)$$

Boudouard:

$$C + CO_2 \rightarrow 2CO \quad (R3)$$

Dry reforming:

$$C_nH_m + nCO_2 \rightarrow 2nCO + (m/2)H_2 \quad (R4)$$

Steam reforming:

$$C_nH_m + nH_2O \rightarrow nCO + (n + m/2)H_2 \quad (R5)$$

$$C_nH_m + 2nH_2O \rightarrow nCO_2 + (m/2+2n)H_2 \quad (R6)$$

Coking reaction:

$$C_nH_m \rightarrow C_nH_x\,(\text{coke}) + (m\text{-}x)/2H_2 \quad (R7)$$

The inherent AAEM particles on the surface of biochar have a crucial role in enhancing the tar reforming process. Ca and K are among the most catalytically active AAEM [20], and their amount are the highest compared to other AAEM in the biochar used for this study (as seen in Table 1). In a high-temperature steam atmosphere, the AAEM species's bond with the char matrix's ("CM") becomes less stable, which leads to the breakage of the bond to generate active sites along with the release of oxygenated (e.g., CO_2) or aliphatic (e.g., CH_4) species [57,58]. These mechanisms can be described by R8 – R9 in the case of K [59]. Thereafter, the released AAEM radicals can combine with the tar fragments, which cause lower stability of the combined tar-AAEM fragments. In a high-temperature, H_2O molecules are ionized to forms O, OH, and H free radicals [44]. These O/H/OH free radicals then can easily replace the AAEM and crack the tar into lighter species. After that, new CM-AAEM bonds can be formed through recombination of the remaining metal species (R10) [59]. The process mentioned above might be one of the reasons that cause the higher measured CO_2 and C_xH_y gases' yield values than their predicted values, especially during co-gasification at higher biochar contents. During the gasification, the tar from waste particles adsorbed into the active char surface, which then increases the repetition of CM-AAEM bond-forming and bond-breaking reactions. Accordingly, more CO_2 and C_xH_y-gases can be generated due to these reactions.

$$(CM—K) = (—CM) + K \quad (R8)$$

$$(—CM) = (—CM') + \text{gas} \quad (R9)$$

$$(—CM') + K = (CM'—K) \quad (R10)$$

Table 3 shows the composition of tar obtained from the SPA/SPE analysis method. As seen in the table, the addition of either biochar or biomass could shift the tar composition. The presence of biochar during gasification of RDF-landfill causes the domination of lighter tars such as benzene (25.6 wt%) and toluene (37.5 wt%); whereas, notable reductions can be observed for heavier tar species such as naphthalene. This finding is in accordance with other studies. According to Zhang et al. [60], biochars have a crucial role in the catalytic cracking of tar, in which they promote the generation of alkyl mono aromatics (e.g., toluene) and inhibit the formation of

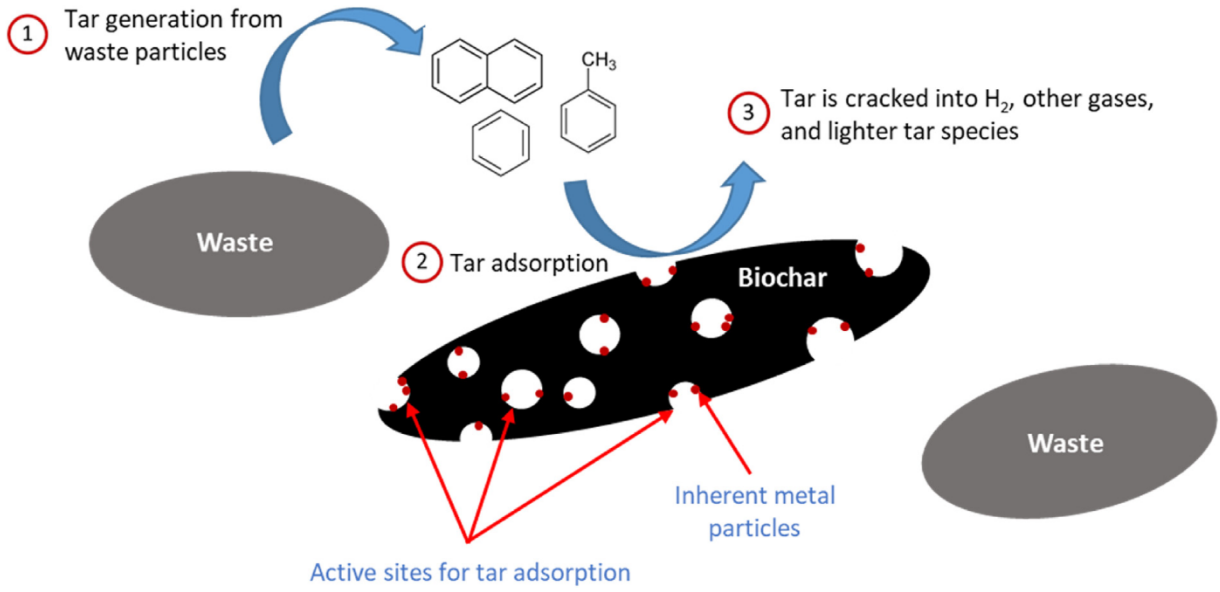

Fig. 5. Illustration of tar reforming mechanisms over biochar during the co-gasification process.

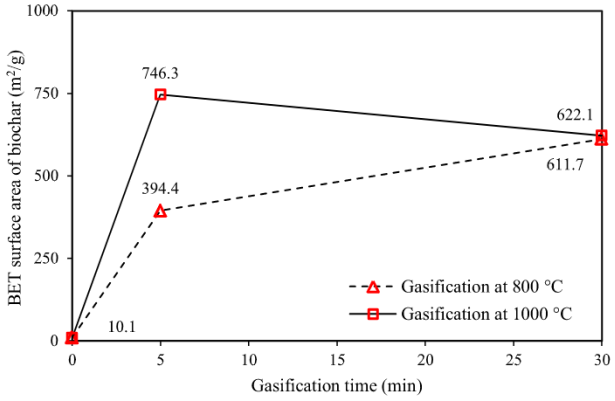

Fig. 6. BET surface area of biochar before and after steam gasification at different temperatures and reaction times.

polycyclic aromatic hydrocarbons (PAH) (e.g., naphthalene). Particularly, the promotion of light tars during co-gasification of RDF-landfill with biochar could be attributed to the role of K. Feng et al. [61] carried out a further investigation on the roles of AAEM on tar reforming with biochar under steam atmosphere. They suggested that K and Ca have different roles in cracking the adsorbed tar molecules. The presence of K is mainly responsible for promoting the in-situ tar cracking into lighter tar species or small-molecule gases, while Ca accounts for combining the tar into biochar structure to achieve the reduction of tar yield. In contrast, the tar produced from the co-gasification of RDF-landfill with biomass exhibits a higher concentration of naphthalene and significant reductions of benzene and toluene's concentrations.

As opposed to the case of co-gasification with biomass, the contribution of a high amount of Si from RDF-landfill does not seem to affect notably the tar cracking performance over biochar. As explained before, the heterogeneous tar conversion over biochar begins when the tar compounds are absorbed into the biochar matrix/pores. Therefore, only the inherent inorganic materials

Table 3
Composition of tar collected through the SPA method during gasification of different fuel mixtures at gasification temperatures of 800 C.

Tar species	Formula	Species concentration in tar sample (wt.%)		
		RDF-landfill	65% RDF-landfill + 35% biomass	65% RDF-landfill + 35% biochar
Benzene	C_6H_6	5.0	0.5	25.6
Toluene	C_7H_8	35.5	1.5	37.5
m/p-Xylene	C_8H_{10}	9.4	3.3	5.1
o-Xylene	C_8H_{10}	15.3	27.9	6.2
Indan	C_9H_{10}	2.1	2.8	1.0
Indene	C_9H_8	6.3	10.7	5.2
Naphthalene	$C_{10}H_8$	12.8	22.1	8.7
2-Methylnaphtalene	$C_{11}H_{10}$	4.5	7.1	2.6
1-Methylnaphtalene	$C_{11}H_{10}$	2.3	4.5	1.6
Biphenyl	$C_{12}H_{10}$	1.4	1.8	1.0
Acenaphthylene	$C_{12}H_8$	0.8	2.7	1.3
Acenaphthene	$C_{12}H_{10}$	1.2	7.8	1.6
Fluorene	$C_{13}H_{10}$	1.7	2.3	1.0
Phenanthrene	$C_{14}H_{10}$	0.8	1.3	1.0
Anthracene	$C_{14}H_{10}$	0.3	0.5	0.3
Fluorantene	$C_{16}H_{10}$	0.1	2.7	0.1
Pyrene	$C_{16}H_{10}$	0.4	0.5	0.3

retained in the interior of the biochar matrix would affect the tar conversion. The external Si particles coming from the RDF-landfill might not have a significant influence as they exist in the form of soil/sand particles. These particles have a larger particle size distribution than the biochar's pores; hence, it can not enter into the biochar matrix without any special treatments.

Table 4 shows the value of the catalytic index for RDF-landfill, biomass, and biochar samples, which are calculated based on the formula proposed by previous studies [62] as seen in Eq. (3). This catalytic index has been used to combine the amount ratio of those catalytic and inhibitor elements and utilize it as a tool to explain the role of the inorganic elements on the gasification performance. As seen in the table, the biochar sample has a lower value than that of biomass, because some of the AAEM species were released during the biochar generation process. Nevertheless, this value is still significantly higher than that of RDF-landfill, and it still indicates the domination of catalytic elements (K, Ca, Mg, Na, and Fe) over the inhibitor elements (Si and Al). Therefore, AAEM can still have significant catalytic effects during the heterogeneous reaction of tar-biochar, despite the higher Si concentration in the biochar matrix.

$$Catalytic\ index = \frac{K + Ca + Mg + Na + Fe}{Si + Al} \quad (3)$$

Overall, raising the gasification temperatures increase the syngas yield regardless of the sample mixtures. In the case of co-gasification with biochar, the rise of syngas yield could be mainly attributed to the higher biochar-steam reaction. This is indicated by the greater conversion rate of the feedstock at higher temperatures (Fig. 4(c)), which rises from only 0.81 to complete conversion of 1.00, as the temperature is elevated from 800 to 1000 °C, respectively. Hence, the gasification produces more H_2 and CO owing to the water gas reaction (R1), which leads to a higher total syngas yield. Additionally, a higher gasification temperature also favors the Boudouard reaction (R3) [32]. Hence, more CO and fewer CO_2 are produced at higher temperatures.

Even though biochar co-gasification results in a lower tar generation than that of biomass, its tar cracking performance decrease at higher gasification temperatures. This phenomenon is mainly caused by the structural change of biochar and the release of AAEM species at higher gasification temperatures. According to Widayatno et al. [63], the promoting effect of tar steam reforming over biochar raises at first and then decreases with the increase of the BET surface area of biochar. It is found that at high values of BET surface area, the content of AAEM species in the biochar could be decreased [63]. This explanation is in accordance with the findings in this study. Fig. 6 illustrates the change in the biochar structure during gasification at different temperatures as indicated by the shifts in its BET surface area value. As seen in the figure, the surface area value increases significantly in the first 5 min of the steam gasification. In specific, the surface area's value during the gasification at 1000 °C is almost doubled (746.3 m^2/g) than that of 800 °C (394.4 m^2/g). Nevertheless, after 30 min of gasification, the surface area of biochar at 1000 °C decreases; whereas, the value increases in the case of 800 °C, which leads to a similar value for both cases. This trend implies that at 1000 °C, the biochar experiences a rapid pore growth at the early stage of the gasification, instead of the latter stage. As seen in Fig. 7(b), mesopores (pore width > 2 nm) already start to emerge after 5 min of gasification at 1000 °C. After 30 min of gasification, the pore volume decrease as the pores collapse with the more consumption of carbon by steam. In contrast, the pore volume distribution of biochar after 5 min of gasification at 800 °C is still dominated by micropores, with no larger pore sizes are detected as seen in Fig. 7(a). As the gasification continues, the pores start to grow and mesopores can be detected in the biochar at the end of gasification test.

The rapid pore enlargement during gasification at higher temperatures consequently causes the release of more AAEM species. Fig. 8 shows the amount of AAEM contents in the biochar after gasification at temperatures of 800 and 1000 °C, which corresponds to the initial mass of the biochar sample. As seen in the figure, there is less amount of AAEM species in the spent biochar after gasification at 1000 °C, than that of 800 °C. Specifically, the amount of Ca, K, Mg, and Na decrease by approximately 11, 38, 7, and 34%, respectively. This trend illustrates that a higher amount of AAEM is released from biochar with the increase of the steam gasification temperature. Correspondingly, the release of AAEM as gaseous species reduces the number of active sites, which leads to the lower rate of tar cracking reactions during co-gasification at higher temperatures.

Additionally, the reduction of tar conversion at 900 and 1000 °C might also be attributed to the higher amount of gases released by the gasification reaction of H_2O with biochar itself, as mentioned

Table 4
The value of the catalytic index for the tested samples.

Samples	Catalytic index's value
RDF-landfill	0.35
Biomass (beech wood)	20.16
Biochar (beech wood char)	16.07

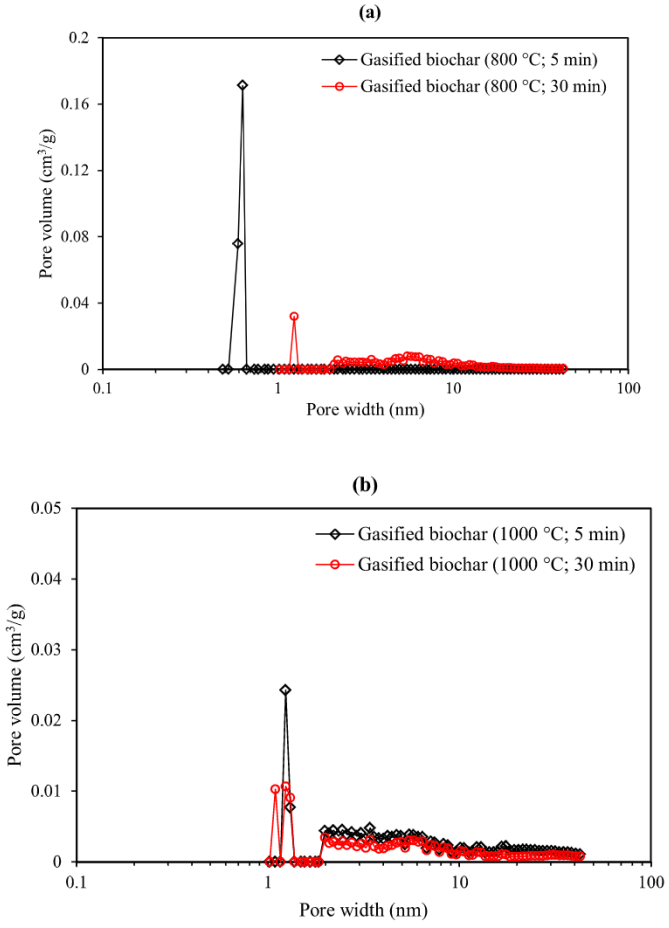

Fig. 7. Pore volume distributions obtained by using the NLDFT method for biochar treated after 5 and 30 min of steam gasification at (a) 800 and (b) 1000 °C.

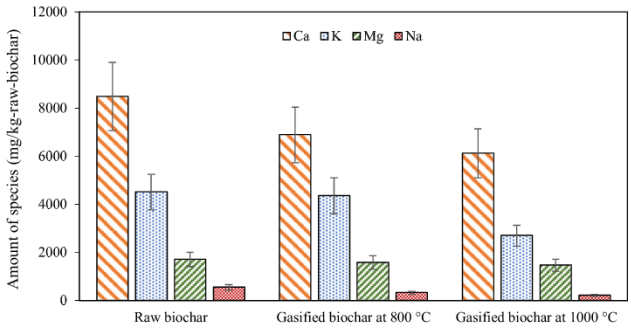

Fig. 8. The amount of AAEM contents in the raw and gasified biochar with respect to the initial mass of raw biochar.

above. Consequently, as there are more gases released from the particle, the diffusion of tar species to the char active sites could be hindered. Hence, more tar species could not be cracked due to the absence of adsorption occurring at the active sites of the char surface.

5. Conclusions

In this study, the potential of biomass or biochar addition during steam co-gasification of RDF obtained from excavated landfill waste to improve its gasification performance is investigated, especially concerning the H_2 yield. The experiments were carried out at biomass or biochar contents of 15, 25, and 35 wt% at a gasification temperature of 800 °C. Fuel mixtures with 35 wt% of biomass/biochar were then subjected to the gasification with temperatures range between 800 and 1000 °C to investigate the effect of temperature. The following conclusions can be made.

1) The addition of biomass can enhance the H_2 yield proportionally with the increase of biomass share. At 800 °C, this result leads to a maximum H_2 concentration of 45.2 vol% at 25 wt% biomass content. No apparent synergetic effects are observed on the H_2 yield during co-gasification, which might cause by the high Si content from RDF-landfill.
2) The addition of biochar produces higher H_2 and total syngas yields than that of biomass co-gasification. The H_2 yield non-linearly increases with the biochar proportion, which indicates the occurrence of synergetic effects. This phenomenon is caused by the tar reforming reactions over biochar particles. At 800 °C, the maximum H_2 concentration of 53.5 vol% is achieved at 35 wt % biochar content. Further H_2 enrichment is obtained at higher temperatures as the concentration reaches 55.8 vol% at 1000 °C.
3) Biochar can effectively reduce more tar amount than that of biomass at low gasification temperatures. However, the tar removal efficiency decreases with increasing gasification temperature, which mainly due to the reduction of active sites of biochar following the release of more AAEM and the higher rate of biochar-steam reactions at higher temperatures.
4) The presence of biomass increases CO production, which causes a lower H_2/CO ratio than that of biochar co-gasification.
5) Both biomass and biochar could improve the efficiency of landfill waste gasification, as indicated by the higher values of the energy yield ratio (EY). Additionally, the results from co-gasifications at higher temperatures indicate higher EY values in the case of gasification using biochar additions.

In general, the addition of biochar shows a promising result for enhancing the gasification performance of landfill waste by increasing its H_2 concentration, syngas yield, and efficiency. Further studies shall be done to optimize the performance by improving biochar porosity, as well as its metal species concentration.

CRediT authorship contribution statement

Ilman Nuran Zaini: Conceptualization, Methodology, Validation, Investigation, Resources, Writing - original draft, Writing - review & editing. **Yamid Gomez-Rueda:** Resources, Writing - review & editing. **Cristina García López:** Resources, Writing - review & editing. **Devy Kartika Ratnasari:** Resources, Writing - review & editing. **Lieve Helsen:** Resources, Writing - review & editing. **Thomas Pretz:** Resources, Writing - review & editing. **Pär Göran Jönsson:** Supervision, Writing - review & editing, Funding acquisition. **Weihong Yang:** Supervision, Writing - review & editing, Funding acquisition.

Declaration of competing interest

The authors declare that they have no known competing financial interests or personal relationships that could have appeared to influence the work reported in this paper.

Acknowledgements

The NEW-MINE project has received funding from the European Union's Horizon 2020 research and innovation programme under the Marie Skłodowska-Curie grant agreement No 721185. Project website: http://new-mine.eu/

References

[1] Jones PT, Geysen D, Tielemans Y, Van Passel S, Pontikes Y, Blanpain B, et al. Enhanced Landfill Mining in view of multiple resource recovery: a critical review. J Clean Prod 2013;55:45–55. https://doi.org/10.1016/j.jclepro.2012.05.021.
[2] Olabi AG. Circular economy and renewable energy. Energy 2019;181:450–4. https://doi.org/10.1016/j.energy.2019.05.196.
[3] EURELCO. Data launched on the landfill situation in the EU-28 2019:1–4. https://eurelco.org/infographic/. [Accessed 8 January 2019].
[4] Laner D, Esguerra JL, Krook J, Horttanainen M, Kriipsalu M, Rosendal RM, et al. Systematic assessment of critical factors for the economic performance of landfill mining in Europe: what drives the economy of landfill mining? Waste Manag 2019;95:674–86. https://doi.org/10.1016/j.wasman.2019.07.007.
[5] Danthurebandara M, Van Passel S, Vanderreydt I, Van Acker K. Assessment of environmental and economic feasibility of enhanced landfill mining. Waste Manag 2014;45:434–47. https://doi.org/10.1016/j.wasman.2015.01.041.
[6] Zaini IN, Nurdiawati A, Aziz M. Cogeneration of power and H2 by steam gasification and syngas chemical looping of macroalgae. Appl Energy 2017;207:134–45. https://doi.org/10.1016/j.apenergy.2017.06.071.
[7] Qadi NMN, Zaini IN, Takahashi F, Yoshikawa K. CO2 co-gasification of coal and algae in a downdraft fixed-bed gasifier: effect of CO2 partial pressure and blending ratio. Energy Fuels 2017;31:2927–33. https://doi.org/10.1021/acs.energyfuels.6b03148.
[8] AlNouss A, McKay G, Al-Ansari T. A comparison of steam and oxygen fed biomass gasification through a techno-economic-environmental study. Energy Convers Manag 2020:208. https://doi.org/10.1016/j.enconman.2020.112612.
[9] Shayan E, Zare V, Mirzaee I. Hydrogen production from biomass gasification; a theoretical comparison of using different gasification agents. Energy Convers Manag 2018;159:30–41. https://doi.org/10.1016/j.enconman.2017.12.096.
[10] Sharma S, Basu S, Shetti NP, Aminabhavi TM. Waste-to-energy nexus for circular economy and environmental protection: recent trends in hydrogen energy. Sci Total Environ 2020;713. https://doi.org/10.1016/j.scitotenv.2020.136633.
[11] Nurdiawati A, Zaini IN, Amin M, Sasongko D, Aziz M. Microalgae-based coproduction of ammonia and power employing chemical looping process. Chem Eng Res Des 2019:311–23. https://doi.org/10.1016/j.cherd.2019.04.013.
[12] Juangsa FB, Aziz M. Integrated system of thermochemical cycle of ammonia, nitrogen production, and power generation. Int J Hydrogen Energy 2019. https://doi.org/10.1016/j.ijhydene.2019.05.110.
[13] Nurdiawati A, Zaini IN, Irhamna AR, Sasongko D, Aziz M. Novel configuration of supercritical water gasification and chemical looping for highly-efficient hydrogen production from microalgae. Renew Sustain Energy Rev 2019;112:369–81. https://doi.org/10.1016/j.rser.2019.05.054.

[14] Shi L, Qi S, Qu J, Che T, Yi C, Yang B. Integration of hydrogenation and dehydrogenation based on dibenzyltoluene as liquid organic hydrogen energy carrier. Int J Hydrogen Energy 2019:5345–54. https://doi.org/10.1016/j.ijhydene.2018.09.083.
[15] International Energy Agency (IEA). The future of hydrogen: seizing today's opportunities. 2019.
[16] Bosmans A, Dobbelaere C De, Helsen L. Pyrolysis characteristics of excavated waste material processed into refuse derived fuel. Fuel 2014;122:198–205. https://doi.org/10.1016/j.fuel.2014.01.019.
[17] Zhou C, Fang W, Xu W, Cao A, Wang R. Characteristics and the recovery potential of plastic wastes obtained from landfill mining. J Clean Prod 2014;80:80–6. https://doi.org/10.1016/j.jclepro.2014.05.083.
[18] Quaghebeur M, Laenen B, Geysen D, Nielsen P, Pontikes Y, Van Gerven T, et al. Characterization of landfilled materials: screening of the enhanced landfill mining potential. J Clean Prod 2013;55:72–83. https://doi.org/10.1016/j.jclepro.2012.06.012.
[19] Materazzi M, Lettieri P, Taylor R, Chapman C. Performance analysis of RDF gasification in a two stage fluidized bed-plasma process. Waste Manag 2016;47:256–66. https://doi.org/10.1016/j.wasman.2015.06.016.
[20] Zaini IN, Lopez CG, Pretz T, Yang W, Jönsson PG. Characterization of pyrolysis products of high-ash excavated-waste and its char gasification reactivity and kinetics under a steam atmosphere. Waste Manag 2019;97pri:149–63. https://doi.org/10.1016/j.wasman.2019.08.001.
[21] Gomez-Rueda Y, Zaini IN, Yang W, Helsen L. Thermal tar cracking enhanced by cold plasma – a study of naphthalene as tar surrogate. Energy Convers Manag 2020;208:112540. https://doi.org/10.1016/j.enconman.2020.112540.
[22] Salem AM, Zaini IN, Paul MC, Yang W. The evolution and formation of tar species in a downdraft gasifier: numerical modelling and experimental validation. Biomass Bioenergy 2019;130:105377. https://doi.org/10.1016/j.biombioe.2019.105377.
[23] Pinto F, André RN, Carolino C, Miranda M, Abelha P, Direito D, et al. Gasification improvement of a poor quality solid recovered fuel (SRF). Effect of using natural minerals and biomass wastes blends. Fuel 2014;117:1034–44. https://doi.org/10.1016/j.fuel.2013.10.015.
[24] Cao Y, Fu L, Mofrad A. Combined-gasification of biomass and municipal solid waste in a fluidized bed gasifier. J Energy Inst 2019:6–11. https://doi.org/10.1016/j.joei.2019.01.006.
[25] Mastellone ML, Zaccariello L, Arena U. Co-gasification of coal, plastic waste and wood in a bubbling fluidized bed reactor. Fuel 2010;89:2991–3000. https://doi.org/10.1016/j.fuel.2010.05.019.
[26] Tanigaki N, Manako K, Osada M. Co-gasification of municipal solid waste and material recovery in a large-scale gasification and melting system. Waste Manag 2012;32:667–75. https://doi.org/10.1016/j.wasman.2011.10.019.
[27] Nippon steel engineering. Direct melting system n.d. https://www.eng.nipponsteel.com/english/whatwedo/wastetoenergy/wtoeplant/direct_melting_system/. [Accessed 16 July 2019].
[28] Nanyang Technological University. NTU and NEA launch unique S$40 million Waste-to-Energy Research Facility. 2019. EurekAlert!, https://www.eurekalert.org/pub_releases/2019-05/ntu-nan052719.php. [Accessed 16 July 2019].
[29] The National Environment Agency. Waste-to-Energy (WTE) test-bedding and demonstration funding initiative 2020 (accessed April 13, 2020), https://www.nea.gov.sg/programmes-grants/grants-and-awards/wte-testbed-demo-initiative.
[30] Zhang Q, Dor L, Zhang L, Yang W, Blasiak W. Performance analysis of municipal solid waste gasification with steam in a Plasma Gasification Melting reactor. Appl Energy 2012;98:219–29. https://doi.org/10.1016/j.apenergy.2012.03.028.
[31] Beagle E, Wang Y, Bell D, Belmont E. Co-gasification of pine and oak biochar with sub-bituminous coal in carbon dioxide. Bioresour Technol 2018;251:31–9. https://doi.org/10.1016/j.biortech.2017.12.027.
[32] Waheed QMK, Wu C, Williams PT. Hydrogen production from high temperature steam catalytic gasi fication of bio-char. J Energy Inst 2016;89:222–30. https://doi.org/10.1016/j.joei.2015.02.001.
[33] Jia S, Ning S, Ying H, Sun Y, Xu W, Yin H. High quality syngas production from catalytic gasi fi cation of woodchip char. Energy Convers Manag 2017;151:457–64. https://doi.org/10.1016/j.enconman.2017.09.008.
[34] Zhai M, Zhang Y, Dong P, Liu P. Characteristics of rice husk char gasification with steam. Fuel 2015;158:42–9. https://doi.org/10.1016/j.fuel.2015.05.019.
[35] Zhai M, Liu J, Wang Z, Guo L, Wang X, Zhang Y, et al. Gasification characteristics of sawdust char at a high-temperature steam atmosphere. Energy 2017;128:509–18. https://doi.org/10.1016/j.energy.2017.04.083.
[36] Sattar A, Leeke GA, Hornung A, Wood J. Steam gasification of rapeseed, wood, sewage sludge and miscanthus biochars for the production of a hydrogen-rich syngas. Biomass Bioenergy 2014;69:276–86. https://doi.org/10.1016/j.biombioe.2014.07.025.
[37] Zhai M, Xu Y, Guo L, Zhang Y, Dong P, Huang Y. Characteristics of pore structure of rice husk char during high-temperature steam gasification. Fuel 2016;185:622–9. https://doi.org/10.1016/j.fuel.2016.08.028.
[38] Yang X, Liu X, Li R, Liu C, Qing T, Yue X, et al. Co-gasification of thermally pretreated wheat straw with Shengli lignite for hydrogen production. Renew Energy 2018;117:501–8. https://doi.org/10.1016/j.renene.2017.10.055.
[39] Shen L, Murakami K. Steam co-gasification of iron-loaded biochar and low-rank coal. Int J Energy Res 2016;40:1846–54. https://doi.org/10.1002/er.3565.
[40] García López C, Ni A, Parrodi JCH, Küppers B, Raulf K, Pretz T. Characterization of landfill mining material after ballistic separation to evaluate material and enery recovery potential. Detritus 2019. https://doi.org/10.31025/2611-4135/2019.13780.
[41] Ratnasari DK, Yang W, Jönsson PG. Kinetic study of an H-ZSM-5/Al-MCM-41 catalyst mixture and its application in lignocellulose biomass pyrolysis. Energy Fuels 2019;33:5360–7. https://doi.org/10.1021/acs.energyfuels.9b00866.
[42] Sophonrat N, Sandström L, Zaini IN, Yang W. Stepwise pyrolysis of mixed plastics and paper for separation of oxygenated and hydrocarbon condensates. Appl Energy 2018;229:314–25. https://doi.org/10.1016/j.apenergy.2018.08.006.
[43] Brage C, Yu Q, Chen G, Sjöström K. Use of amino phase adsorbent for biomass tar sampling and separation. Fuel 1997;76:137–42. https://doi.org/10.1016/S0016-2361(96)00199-8.
[44] Saad JM, Williams PT. Manipulating the H2/CO ratio from dry reforming of simulated mixed waste plastics by the addition of steam. Fuel Process Technol 2017;156:331–8. https://doi.org/10.1016/j.fuproc.2016.09.016.
[45] Ahmed II, Nipattummakul N, Gupta AK. Characteristics of syngas from co-gasification of polyethylene and woodchips. Appl Energy 2011;88:165–74. https://doi.org/10.1016/j.apenergy.2010.07.007.
[46] Burra KG, Gupta AK. Synergistic effects in steam gasification of combined biomass and plastic waste mixtures. Appl Energy 2018;211:230–6. https://doi.org/10.1016/j.apenergy.2017.10.130.
[47] Lopez G, Erkiaga A, Amutio M, Bilbao J, Olazar M. Effect of polyethylene co-feeding in the steam gasification of biomass in a conical spouted bed reactor. Fuel 2015;153:393–401. https://doi.org/10.1016/j.fuel.2015.03.006.
[48] Deng L, Zhang T, Che D. Effect of water washing on fuel properties, pyrolysis and combustion characteristics, and ash fusibility of biomass. Fuel Process Technol 2013;106:712–20. https://doi.org/10.1016/j.fuproc.2012.10.006.
[49] Vamvuka D, Sfakiotakis S. Effects of heating rate and water leaching of perennial energy crops on pyrolysis characteristics and kinetics. Renew Energy 2011;36:2433–9. https://doi.org/10.1016/j.renene.2011.02.013.
[50] Rizkiana J, Guan G, Widayatno WB, Hao X, Li X, Huang W, et al. Promoting effect of various biomass ashes on the steam gasification of low-rank coal. Appl Energy 2014;133:282–8. https://doi.org/10.1016/j.apenergy.2014.07.091.
[51] Shen Y. Chars as carbonaceous adsorbents/catalysts for tar elimination during biomass pyrolysis or gasification. Renew Sustain Energy Rev 2015;43:281–95. https://doi.org/10.1016/j.rser.2014.11.061.
[52] Shen Y, Fu Y. Advances in: in situ and ex situ tar reforming with biochar catalysts for clean energy production. Sustain Energy Fuels 2018;2:326–44. https://doi.org/10.1039/c7se00553a.
[53] Ates F, Tezcan Un U. Production of char from hornbeam sawdust and its performance evaluation in the dye removal. J Anal Appl Pyrolysis 2013;103:159–66. https://doi.org/10.1016/j.jaap.2013.01.021.
[54] Han T, Lu X, Sun Y, Jiang J, Yang W, Jönsson PG. Magnetic bio-activated carbon production from lignin via a streamlined process and its use in phosphate removal from aqueous solutions. Sci Total Environ 2020:708. https://doi.org/10.1016/j.scitotenv.2019.135069.
[55] Fu P, Yi W, Li Z, Bai X, Wang L. Evolution of char structural features during fast pyrolysis of corn straw with solid heat carriers in a novel V-shaped down tube reactor. Energy Convers Manag 2017;149:570–8. https://doi.org/10.1016/j.enconman.2017.07.068.
[56] Xie Y, Zeng K, Flamant G, Yang H, Liu N, He X, et al. Solar pyrolysis of cotton stalk in molten salt for bio-fuel production. Energy 2019;179:1124–32. https://doi.org/10.1016/j.energy.2019.05.055.
[57] Li CZ, Sathe C, Kershaw JR, Pang Y. Fates and roles of alkali and alkaline earth metals during the pyrolysis of a Victorian brown coal. Fuel 2000;79:427–38. https://doi.org/10.1016/S0016-2361(99)00178-7.
[58] Sathe C, Pang Y, Li CZ. Effects of heating rate and ion-exchangeable cations on the pyrolysis yields from a Victorian brown coal. Energy Fuels 1999;13:748–55. https://doi.org/10.1021/ef980240o.
[59] Li CZ. Some recent advances in the understanding of the pyrolysis and gasification behaviour of Victorian brown coal. Fuel 2007;86:1664–83. https://doi.org/10.1016/j.fuel.2007.01.008.
[60] Zhang YL, Wu WG, Zhao SH, Long YF, Luo YH. Experimental study on pyrolysis tar removal over rice straw char and inner pore structure evolution of char. Fuel Process Technol 2015;134:333–44. https://doi.org/10.1016/j.fuproc.2015.01.047.
[61] Feng D, Zhao Y, Zhang Y, Zhang Z, Sun S. Roles and fates of K and Ca species on biochar structure during in-situ tar H2O reforming over nascent biochar. Int J Hydrogen Energy 2017;42:21686–96. https://doi.org/10.1016/j.ijhydene.2017.07.096.
[62] Bouraoui Z, Jeguirim M, Guizani C, Limousy L, Dupont C, Gadiou R. Thermogravimetric study on the influence of structural, textural and chemical properties of biomass chars on CO2 gasification reactivity. Energy 2015;88:703–10. https://doi.org/10.1016/j.energy.2015.05.100.
[63] Widayatno WB, Guan G, Rizkiana J, Hao X, Wang Z, Samart C, et al. Steam reforming of tar derived from Fallopia Japonica stem over its own chars prepared at different conditions. Fuel 2014;132:204–10. https://doi.org/10.1016/j.fuel.2014.04.089.